THE JOURNAL OF PHYSICAL CHEMISTRY C LETTERS

2008, *112*, 20105–20108
Published on Web 11/24/2008

Uniform *N*-(2-Aminoethyl)(3-aminopropyl)trimethoxysilane Monolayer Growth in Water

Jing Zhang, Johan Hoogboom, Paul H. J. Kouwer, Alan E. Rowan, and Theo Rasing*

Institute for Molecules and Materials, Radboud University Nijmegen, Heyendaalseweg 135, 6525AJ, Nijmegen, The Netherlands

Received: June 16, 2008; Revised Manuscript Received: August 14, 2008

The commonly preferred approach to grow silane self-assembled monolayers (SAMs), using anhydrous solvents while maintaining some absorbed water at the solid substrates, is difficult to control and very often leads to irreproducibility. In the search for a new approach for functional hydrophilic monolayers, we tested water as a solvent for monolayer growth. As a model system, we investigated monolayer growth of *N*-(2-aminoethyl)(3-aminopropyl)trimethoxysilane (EDA) in water at various silane concentrations and temperatures. The topology and the thickness of the EDA layers were measured by atomic force microscopy and ellipsometry respectively; their molecular properties were studied by using liquid crystals as an optical amplification probe. We found that growth at low silane concentrations and low temperatures resulted in uniform monolayers. This makes our method of considerable interest for the construction of (bio)functionalized surfaces that require the use of aqueous media.

Introduction

Modification of solid surfaces with silane self-assembled monolayers (SAMs) has been shown to be important for a wide range of organic molecular devices.[1] Despite extensive research devoted to this field, uniform silane monolayers are still difficult to obtain,[2−4] mainly due to the competing polymerization process of multifunctional silanes in the bulk and subsequent absorption on the substrate, resulting in poorly defined multilayer structures.[5] An efficient approach to circumvent this problem is the use of monofunctional silanes; however, the observation that trifunctional silanes are chemically more robust than their monofunctional counterparts[2,6,7] prompted us to study trifunctional silanes.

In solution, silanes are hydrolyzed by water to silanols (hydrolysis reaction) before they covalently bind to hydroxyl-covered solid surfaces or polymerize (condensation reaction).[4,6,8] The conventional approach to uniform silane monolayer growth therefore avoids water in the bulk solution and employs the adsorbed water layer on the solid substrates for hydrolysis.[2,4] This approach relies on the subtle control of the amount and location of water molecules, which is difficult to control in practice. First, the amount of adsorbed water on solid substrates is dependent on humidity and temperature. Second, the adsorbed water molecules on the solid substrates will diffuse into the bulk solution while the substrates are in the solution, especially when polar silanes and polar solvents are used. This approach therefore often gives rise to poor reproducibility.[2−5,9]

In this paper, we present our results on monolayer growth of a hydrophilic silane *N*-(2-aminoethyl)(3-aminopropyl)trimethoxysilane (EDA) in pure water at various temperatures and concentrations. Although this approach is limited to water soluble silanes, the use of water will bypass any reproducibility problems. On top of that, this approach is highly interesting for the direct functionalization of surfaces with biomaterials that require aqueous conditions; these surfaces are now commonly obtained by a postmodification step of an (amine) functionalized surface.

* To whom correspondence should be addressed. E-mail: th.rasing@science.ru.nl.

Experiment and Results

Sample Preparation. The substrates for the EDA layer growth were cut from objective glass slides (Knittel Glaser). They were ultrasonically cleaned with detergent (ALCONOX), 1 M NaOH (99%, Merck) for 10 min each, rinsed with copious amounts of tap water, and then ultrasonically cleaned with two times refreshed demi-water and two times refreshed MilliQ-water and acetone (99.8%, Merck) for 10 min each. At last, they were blown dry with N_2 and cleaned with a UV/ozone cleaner (Novascan Technologies, Inc.) for 10 min.

EDA (≥98%, Aldrich Chemical Co.) was air-seal stored and transferred to solution in N_2 (grade 6.0) flow to prevent any prereaction with air moisture. Different concentrations of EDA in MilliQ-water were prepared in presilanized glass bottles. The substrates were immersed in each EDA solution immediately after it was prepared. The bottles were then sealed and stored in a thermostat for 3 days to allow the SAM growth to reach completion. The substrates were then ultrasonically rinsed in three times refreshed MilliQ-water and isopropyl alcohol (99.7%, Merck) for 5 min each to remove any noncovalently bonded molecules. Finally, the substrates were blown dry with N_2.

AFM Measurements. The topology of the samples was studied by an atomic force microscope (AFM, Dimension 3100, Veeco). The AFM images were obtained using a Silicon tip (NSG10, NT-MDT) scanned in tapping mode under ambient air. All the measurements were done immediately after the samples were prepared. Figure 1a−e shows the AFM images ($5 \times 5\ \mu m$) of the samples (a−e) grown at a fixed temperature of 35.0 °C and various initial silane concentrations: (a) 0.01 mM, (b) 0.05 mM, (c) 0.5 mM, (d) 10 mM, and (e)100 mM. The corresponding root-mean-square roughness (rms) of these samples increases from 0.20 ± 0.06 nm (for a,b) to 0.81, 0.98, and 1.30 nm (for c−e, respectively). Similar results were

10.1021/jp805283u CCC: $40.75

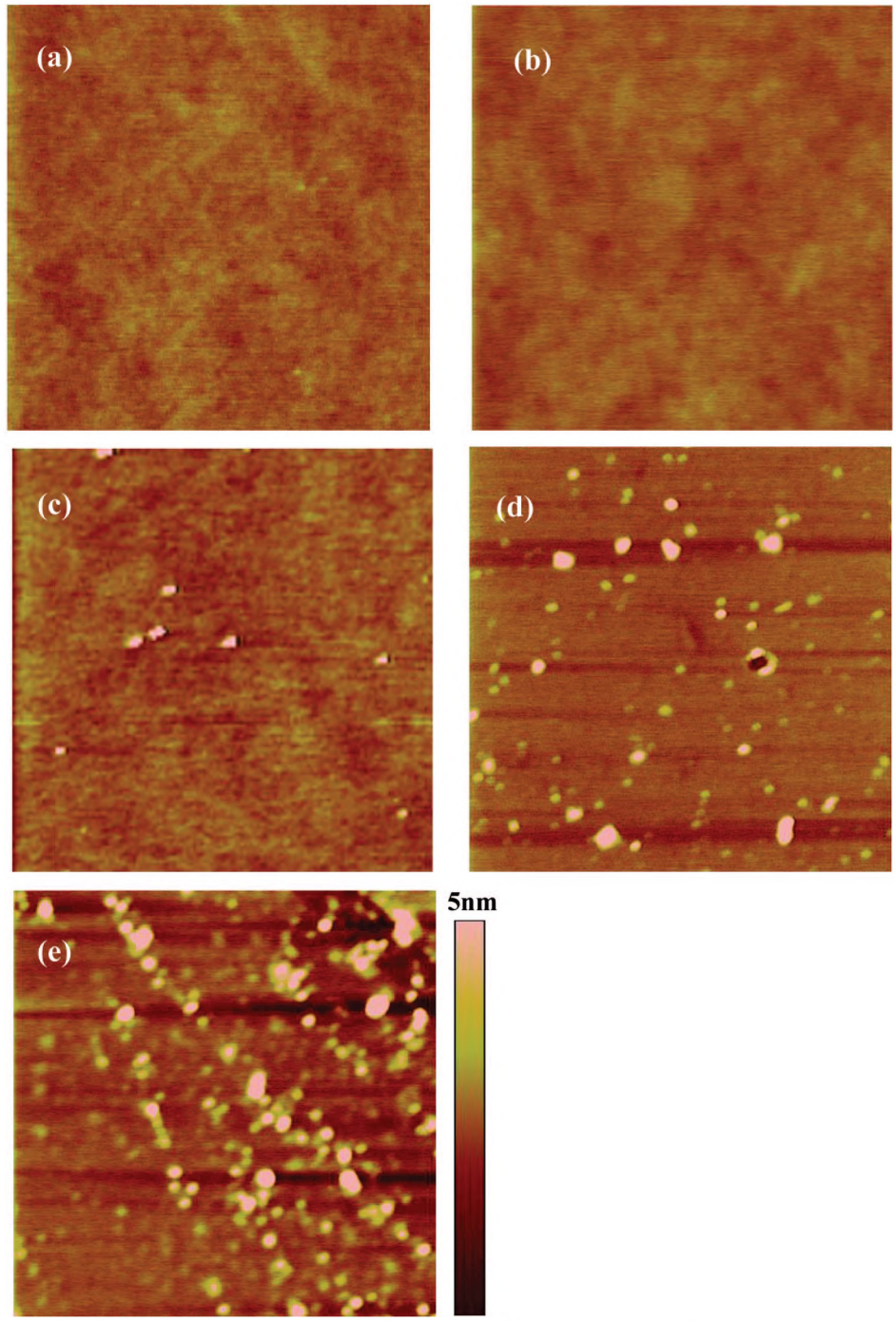

Figure 1. AFM images of EDA samples grown at 35 °C and various concentrations: (a) 0.01 mM, (b) 0.05 mM, (c) 0.5 mM, (d) 10 mM, (e) 100 mM. All the images are 5 μm $\times$ 5 μm in size and shown with the same color scale as panel e.

obtained for samples grown at 27.5 and 20.0 °C. Figure 2 shows the rms of all the measured samples. Since the rms of the glass substrates vary from piece to piece within 0.20 $\pm$ 0.06 nm under the same AFM measurement conditions (512 $\times$ 512 pixels over 5 $\times$ 5 μm), samples with the same rms values as the substrates were considered as smooth layers and samples with an rms above that of the substrates were considered as rough layers. Accordingly, all the measured samples were separated into two groups by a separation line in Figure 2.

Ellipsometry Measurements. The thickness of the EDA layers was studied by a spectroscopic ellipsometer VB-400 (J. A. Woollam Co., Inc.) using equally smooth but reflective substrates, which were cut from a single crystal Si (100) wafer capped by a native SiO_2 layer. The substrates were cleaned with the same procedure as that for the glass substrates. Bare substrates and EDA samples were measured at 60, 70, and 80° incident angles and scanned from 500 to 1000 nm wavelength at each incident angle in order to collect a large enough data set for fitting purposes. All the fitting was done by commercial software WVASE32 (J. A. Woollam Co., Inc.). The thickness of the SiO_2 layer was obtained by fitting the data set with a two layer model. The thickness of the EDA layers was obtained by fitting a third layer on top of the measured SiO_2 layer. Since EDA is nonabsorbing in the measured wavelength range, the refractive index dispersion of EDA was fitted with a Cauchy model $n = A + B(1/\lambda^2)$, where $A = 1.44$ for liquid EDA was obtained from literature[10] and $B = 0.007$ μm^2 was fitted from our measurements. This thickness determined by ellipsometry

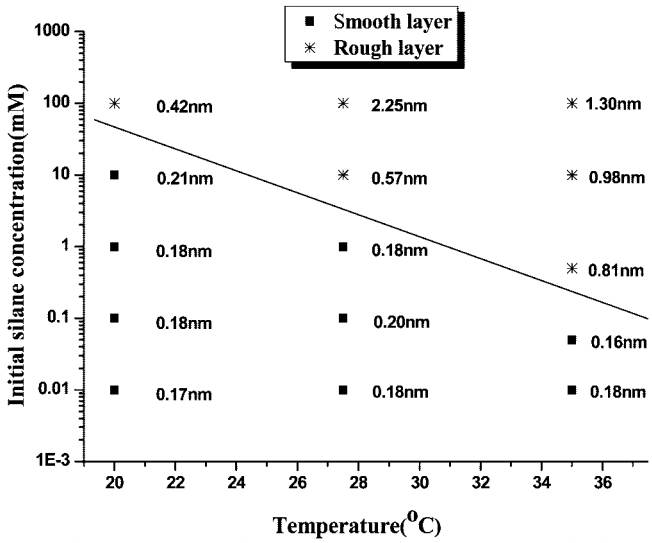

Figure 2. rms of EDA layers grown in pure water at various temperatures and concentrations. The number next to the measured point is the rms value of the EDA layer grown at that condition. Layers with rms within 0.20 ± 0.06 nm are considered as smooth layers and layers with rms above 0.20 ± 0.06 nm are considered as rough layers. The separation line between smooth and rough layers is merely a guide to the eye.

measurements has an inherent limitation in accuracy of ±0.2 nm because of the choice of refractive index for the EDA layers,[10] which is much larger than our measurement error ±0.1 nm. Two typical smooth layers (grown at 20 °C, 0.1 mM and 35 °C, 0.05 mM) were measured to have the same thickness 0.6 ± 0.2 nm. A typical rough EDA layer (grown at 35 °C, 10 mM) was measured to have a mean thickness of 1.5 ± 0.2 nm.

Liquid Crystal Studies. The molecular properties of our samples, in particular their surface terminal groups, were studied by using liquid crystals (LCs) as an optical amplification tool. LCs have been demonstrated to be a sensitive tool for the study of the molecular ordering of SAM surfaces.[11,12] The basic principle of this approach is as follows: if the terminal groups of the SAM molecules, which are normal to the surface, orient the optical axis of LC molecules homeotropically (i.e., normal to the surface), small zenithal deviations of the surface terminal groups will be amplified to the LC bulk of a few micrometers thick across the cell, due to the long-range correlation length of LCs. Therefore, the orientation and uniformity of the terminal groups of SAMs can be studied by studying the bulk LC orientation and alignment uniformity with a polarizing optical microscope.[11,12] Since amine-terminated SAM surfaces are known to align liquid crystal 4-pentyl-4′-cyanobiphenyl (5CB) homeotropically[13,14] via hydrogen bonding under <40% humidity,[14] we used 5CB (Merck) to study the molecular properties of our EDA layers under <35% humidity. The LC cells were made by separating two solid substrates with 4 μm spacers (Licristar, Merck). The cells and 5CB were heated to above T_{IN} = 35 °C, and the cells were then filled with 5CB by capillary force. After that, the filled cells were slowly cooled down to room temperature. The alignment of LCs in the cells was studied by using a polarizing optical microscope (BX60, Olympus). The polarizers of the microscope were adjusted to crossed position (complete extinction) before the LC cells were placed on the sample stage. The images of the LC cells were captured by using a CCD camera and image processing software (Image-Pro Plus 4.0). Figure 3 shows the polarized optical images of LCs sandwiched between different surfaces, and they correspond to different alignment configurations of the LCs: (a) random alignment of LCs when they are in contact with two bare glass surfaces; (b) uniform homeotropic alignment of LCs when in contact with two smooth EDA-covered glass surfaces (the same uniform homeotropic alignment of LCs was observed for all the smooth EDA samples defined in Figure 2) (c) nonuniform homeotropic alignment of LCs in contact with two rough EDA-covered glass surfaces (grown at 35 °C and 10 mM), showing a large number of defects.

Discussion

Figure 2 shows that the samples grown at low concentrations and low temperatures are topologically smooth, while samples grown at higher concentrations and higher temperatures are rough. Smooth samples as shown in Figure 1a,b are topologically indistinguishable from the glass substrates (both have the same rms value of 0.2 ± 0.06 nm). The ellipsometry measurements indicate the presence of an EDA film with a thickness of 0.6 ± 0.2 nm for the smooth samples, which corresponds well to the expected thickness of ~0.8 nm of a densely packed monolayer of EDA molecules normal to the surface. Further LC studies on these smooth sample surfaces show that they are chemically different from the bare substrates. The schlieren texture of nematic LCs appearing in Figure 3a suggests that the LCs are in micron size nematic domains that are aligned randomly on the glass substrates; the complete extinction of light shown in Figure 3b suggests that the LC molecules are aligned homeotropically and uniformly on the smooth EDA-covered samples. Since amino groups are known to align 5CB LC molecules homeotropically by hydrogen bonding, the above observations suggest that the smooth EDA monolayers are terminated with amino groups, which is different from the hydroxyl termination of the glass substrates. Considering the symmetry of the EDA molecule, this amino termination of the smooth EDA layers suggests that they are monolayers. Considering the LC alignment change with the change of the monolayer density, it has been shown that mesoscopic changes of the monolayers, such as from 2D gas to 2D liquid phase transitions or 2D condensed tilted domain formations at the water−nematic interfaces, give locally surface-induced alignment changes of LCs.[12] Therefore, the uniform homeotropic alignment of 5CB LCs observed on our smooth EDA surfaces suggests that these monolayers are relatively densely packed with an average orientation of the terminal amino groups normal to the surface.

The AFM images shown in Figure 1c−e of the rough samples indicate that particles of random sizes and shapes are absorbed on the surfaces. The measured mean thickness of 1.5 ± 0.2 nm of a rough sample (grown at 35 °C and 10 mM) suggests that this sample has on average more than one EDA monolayer. Considering that all the samples were ultrasonically rinsed in three times refreshed MilliQ-water and isopropyl alcohol for 5 min each and then blown dry with N_2 after the solution growth, those particles are very likely to be chemisorbed EDA polymers. The chemisorbed EDA polymers as shown in Figure 1d can be seen to induce alignment defects in LCs as shown in Figure 3c, and those defects are randomly distributed in the homeotropically aligned LC background. Notice that the sample shown in Figure 1c, which has a very low density of absorbed polymers, still gives a uniform homeotropical alignment of the LC phase. These two observations suggest that only surface areas with a locally high density of absorbed polymers give alignment defects in the LCs. This is consistent with the point that mesoscopic changes of the surface give locally surface-induced alignment changes of LCs. In this way, the LCs act as an optical amplification probe of the mesoscopic characteristics of surfaces, which has been demonstrated in many LC-based chemical sensors.[15]

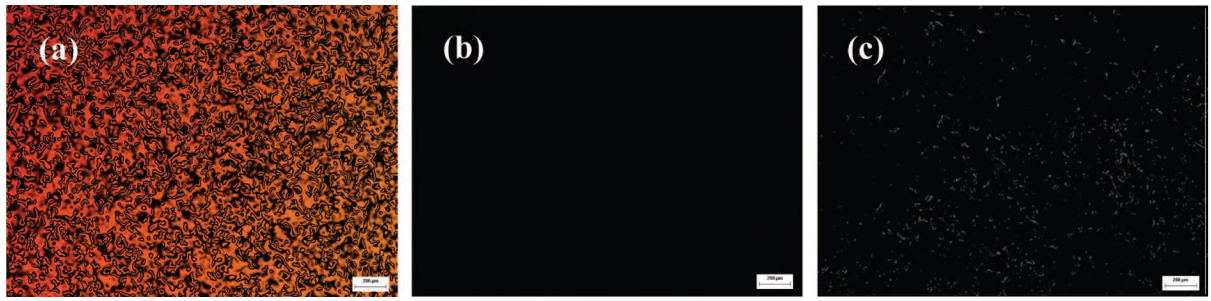

Figure 3. (a−c) Polarizing optical microscopy images of LC cells (transmission mode through crossed polarizers): (a) random azimuthal alignment of LCs in contact with two bare glass surfaces; (b) uniform homeotropical alignment of LCs in contact with two smooth EDA surfaces; (c) nonuniform homeotropical alignment of LCs in contact with two rough EDA surfaces (grown at 35 °C, 10 mM). The scale bars in all the images are 200 μm.

Thus, we can conclude that the smooth EDA SAMs are formed by chemisorption of monomers on the solid substrates while the rough EDA layers are formed by chemisorption of both monomers and polymers. Figure 2 indicates that monomer chemisorption is favored over polymer chemisorption at lower concentrations and this concentration range decreases exponentially with increasing temperature. For a full kinetic model, the temperature and silane concentration dependence of monomer chemisorption versus polymerization and polymer chemisorption should be determined. Kinetic studies to unravel this complex system are currently in progress. Qualitatively, our results can be explained by comparing standard reaction rates of polymerization and surface chemisorption. As our solvent is water, it is reasonable to assume that the hydrolysis of EDA is not the rate limiting step for the condensation reaction. That means silanol concentration is proportional to initial silane concentration. As polymerization requires at least two silanol molecules, its reaction rate is expected to be the second order in the silanol concentration. On the other hand, surface chemisorption is expected to follow the first order kinetics in the silanol concentration.[16] Consequently, at low initial silane concentrations monomer surface adsorption will be much faster than polymerization in the bulk. This strongly reduces the chance of polymer surface adsorption and thus smooth monolayer growth is kinetically favored; see the concentration effect in Figure 2. When the temperature increases, the silanol population, which has enough energy to cross the activation barrier, increases exponentially. That gives a similar effect as exponential increase of the initial silane concentration; see the temperature effect in Figure 2. However, silane concentration and temperature could influence other processes as well, such as physisorption, reverse chemical reactions, etc. Further kinetic studies are needed to fully understand the concentration and temperature effect in silane monolayer growth.

Conclusions

In conclusion, we have demonstrated that uniform SAMs of a hydrophilic silane EDA can be conveniently grown in water. This approach is of considerable interest for the construction of (bio)functionalized surfaces that require the use of aqueous media. We found that the conditions for uniform SAM growth are in a regime of low silane concentration and low temperatures. AFM measurements show that those uniform SAMs are topologically as smooth as the substrates. Ellipsometry measurements suggest that they are densely packed monolayers. Liquid crystal studies indicate that they are molecularly well ordered with their terminal amino groups normal to the surface. Currently, we are using our approach for the surface fictionalization by other strongly hydrophilic molecules like biologically relevant carbohydrates and peptides.

Acknowledgment. We thank Jan W. Gerritsen for help with the AFM measurements, Dr. Elena Mishina for help with the ellipsometry measurements, and Dr. Peter Schön for helpful discussions. We acknowledge financial support from the Dutch NanoNed program.

References and Notes

(1) (a) Kubono, A.; Kyokane, Y.; Kasajima, Y.; Akiyama, R.; Tanaka, K. *J. Appl. Phys.* **2001**, *89* (7), 3554. (b) Ho, P. K. H.; Granstrom, M.; Friend, R. H.; Greenham, N. C. *Adv. Mater.* **1998**, *10* (10), 769. (c) Cornil, D.; Olivier, Y.; Geskin, V.; Cornil, J. *Adv. Funct. Mater.* **2007**, *17* (7), 1143. (d) Kumaki, D.; Ando, S.; Shimono, S.; Yamashita, Y.; Umeda, T.; Tokito, S. *Appl. Phys. Lett.* **2007**, *90* (5), 053506. (e) Chua, L. L.; Zaumseil, J.; Chang, J. F.; Ou, E. C. W.; Ho, P. K. H.; Sirringhaus, H.; Friend, R. H. *Nature* **2005**, *434* (7030), 194. (f) Cahen, D.; Naaman, R.; Vager, Z. *Adv. Funct. Mater.* **2005**, *15* (10), 1571.

(2) Onclin, S.; Ravoo, B. J.; Reinhoudt, D. N. *Angew. Chem., Int. Ed.* **2005**, *44* (39), 6282.

(3) Schreiber, F. *J. Phys.: Condens. Matter* **2004**, *16* (28), R881.

(4) Schwartz, D. K. *Annu. Rev. Phys. Chem.* **2001**, *52*, 107.

(5) Chow, B. Y.; Mosley, D. W.; Jacobson, J. M. *Langmuir* **2005**, *21* (11), 4782.

(6) Waddell, T. G.; Leyden, D. E.; Debello, M. T. *J. Am. Chem. Soc.* **1981**, *103* (18), 5303.

(7) Krumpfer, J. W.; Fadeev, A. Y. *Langmuir* **2006**, *22* (20), 8271.

(8) (a) *Silane Coupling Agents*; Plueddemann, E. P., Ed.; Plenum Press: New York, 1991. (b) Osterholtz, F. D.; Pohl, E. R. *J. Adhes. Sci. Technol.* **1992**, *6* (1), 127.

(9) Brzoska, J. B.; Benazouz, I.; Rondelez, F. *Langmuir* **1994**, *10* (11), 4367.

(10) Stenger, D. A.; Georger, J. H.; Dulcey, C. S.; Hickman, J. J.; Rudolph, A. S.; Nielsen, T. B.; Mccort, S. M.; Calvert, J. M. *J. Am. Chem. Soc.* **1992**, *114* (22), 8435.

(11) Fang, J. Y.; Gehlert, U.; Shashidar, R.; Knobler, C. M. *Langmuir* **1999**, *15* (2), 297.

(12) (a) Brake, J. M.; Daschner, M. K.; Abbott, N. L. *Langmuir* **2005**, *21* (6), 2218. (b) Price, A. D.; Schwartz, D. K. *J. Phys. Chem. B* **2007**, *111* (5), 1007.

(13) Israel, B. A.; Murphy, C. J.; Abbott, N. L. *Nanotechnology* **2005**, *1*, 108.

(14) Kubono, A.; Onoda, H.; Inoue, K.; Tanaka, K.; Akiyama, R. *Mol. Cryst. Liq. Cryst.* **2002**, *373*, 127.

(15) (a) *Surface and Interfaces of Liquid Crystals*; Rasing, T., Musevic, I., Eds.; Springer: New York, 2004. (b) Woltman, S. J.; Jay, G. D.; Crawford, G. P. *Nat. Mater.* **2007**, *6* (12), 929. (c) Hoogboom, J.; Clerx, J.; Otten, M. B. J.; Rowan, A. E.; Rasing, T.; Nolte, R. J. M. *Chem. Commun.* **2003**, (23), 2856. (d) Hoogboom, J.; Velonia, K.; Rasing, T.; Rowan, A. E.; Nolte, R. J. M. *Chem. Commun.* **2006**, (4), 434.

(16) (a) Cheng, S. S.; Scherson, D. A.; Sukenik, C. N. *J. Am. Chem. Soc.* **1992**, *114* (13), 5436. (b) Richter, A. G.; Durbin, M. K.; Yu, C. J.; Dutta, L. *Langmuir* **1998**, *14* (21), 5980. (c) Richter, A. G.; Yu, C. J.; Datta, A.; Kmetko, J.; Dutta, P. *Phys. Rev. E* **2000**, *61* (1), 607.

JP805283U